THE JOURNAL OF BIOLOGICAL CHEMISTRY VOL. 283, NO. 32, pp. 22206–22214, August 8, 2008

SoxAX Cytochromes, a New Type of Heme Copper Protein Involved in Bacterial Energy Generation from Sulfur Compounds*[S]

Received for publication, January 14, 2008, and in revised form, May 29, 2008 Published, JBC Papers in Press, June 14, 2008, DOI 10.1074/jbc.M800315200

Ulrike Kappler[‡§1], Paul V. Bernhardt[‡§], James Kilmartin[‡§], Mark J. Riley[‡§], Julia Teschner[‡2], Kirsty J. McKenzie[‡], and Graeme R. Hanson[§¶]

From the [‡]School of Molecular & Microbial Sciences, the [§]Center for Metals in Biology, and the [¶]Center for Magnetic Resonance, The University of Queensland, Brisbane, Queensland 4072, Australia

SoxAX cytochromes are essential for the function of the only confirmed pathway for bacterial thiosulfate oxidation, the so-called "Sox pathway," in which they catalyze the initial formation of a S–S bond between thiosulfate and the SoxYZ carrier protein. Our work using the *Starkeya novella* diheme SoxAX protein reveals for the first time that in addition to two active site heme groups, SoxAX contains a mononuclear Cu^{II} center with a distorted tetragonal geometry and three to four nitrogen ligands, one of which is a histidine. The Cu^{II} center enhanced SoxAX activity in a newly developed, glutathione-based assay system that mimics the natural reaction of SoxAX with SoxYZ. EPR spectroscopy confirmed that the SoxAX Cu^{II} center is reduced by glutathione. At pH 7 a $K_{m\ app}$ of 0.19 ± 0.028 mM and a $k_{cat\ app}$ of 5.7 ± 0.25 s^{-1} were determined for glutathione. We propose that SoxAX cytochromes are a new type of heme-copper proteins, with SoxAX-mediated S–S bond formation involving both the copper and heme centers.

SoxAX cytochromes are critical for bacterial thiosulfate oxidation via the Sox-multienzyme complex (1–4). To date, this "Sox pathway" is the only confirmed pathway for the oxidation of thiosulfate to sulfate by bacteria as part of the biogeochemical sulfur cycle (5, 6). It was first discovered in *Paracoccus versutus* (7), an aerobic sulfur-oxidizing bacterium, but recent investigations in phototrophic sulfur-oxidizing microorganisms (2, 8) and analysis of published microbial genomes (9) have shown that the Sox pathway and variations thereof are also present in many bacterial species (*e.g. Nitrobacter*, *Dechloromonas*, and *Ralstonia*) that had so far not been associated with this type of metabolism (1). At present, there are ~90 SoxAX-related protein sequences available in public data bases, and this number continues to increase. Together, this indicates that Sox complex-mediated sulfur oxidation is a phylogenetically old process and is of high significance for sulfur transformations in diverse terrestrial and aquatic microbial communities.

The Sox multienzyme complex comprises four essential proteins, a SoxAX cytochrome (4), a SoxYZ carrier protein (10), SoxB (10, 11), and a SoxCD sulfur dehydrogenase (12, 13), all of which are required for oxidation of thiosulfate by this enzyme complex. Several accessory Sox proteins are known but do not appear to be essential for basic complex function (6). Although an overall model of the Sox complex-mediated reaction exists (5, 14), details of the function and reaction mechanisms of each of the four essential Sox proteins are mostly unknown. SoxAX has a crucial function in the Sox complex because it initiates the reaction cycle.

SoxAX cytochromes are heterodimeric proteins with either two or three *c*-type hemes (1, 2, 14, 15). In all cases, a His/Met-ligated heme group is present in SoxX, whereas the SoxA subunit can contain either one or two His/Cys-ligated heme groups. The His/Cys-ligated heme group located close to the SoxX heme in the SoxAX active site is present in all SoxA proteins. In diheme SoxA proteins a second, noncatalytic SoxA heme group is located at a distance of ~24 Å from the active site and has been replaced by a disulfide bond in the monoheme SoxA proteins such as the one from our model organism, *Starkeya novella* (1, 15).

Crystal structures of two closely related triheme SoxAX proteins (14, 16) have revealed another intriguing detail; in both cases, the cysteine ligand of the active site SoxA heme group was modified to a cysteine persulfide that has been attributed to incomplete reaction cycles or degradation of a thiosulfate molecule bound to the cysteine during purification (14).

However, it appears that persulfide modification is not the only modification state that the SoxA active site cysteine can assume. Following exposure to both inorganic and organosulfur compounds, the mass fingerprint of the *S. novella* SoxA subunit was altered (17), and increases by 32, 80, and 112 Da, corresponding to the masses of a sulfur atom, a sulfite, and a thiosulfate anion, respectively, were observed (17). Interestingly, exposure to its proposed substrate, thiosulfate, did not appear to cause changes in the SoxA mass fingerprint.

SoxAX cytochromes are also notable for their complex EPR spectra where four low spin Fe^{III} heme-dependent EPR signals (LS1a,b, LS2, and LS3) are observed for both di- and triheme SoxAX proteins (1, 17, 18). Although LS3 is associated with the His/Met-ligated heme in SoxX, LS1a,b and LS2 are thought to

* This work was supported by a grant and fellowship from the University of Queensland (to U. K.) and by Australian Research Council Linkage Infrastructure Equipment and Facilities Grant LE0344441. The costs of publication of this article were defrayed in part by the payment of page charges. This article must therefore be hereby marked "*advertisement*" in accordance with 18 U.S.C. Section 1734 solely to indicate this fact.

[S] The on-line version of this article (available at http://www.jbc.org) contains supplemental Table S1 and Figs. S1–S3.

[1] Present address: Biozentrum, Spielmannstrasse 7, Technische Universität Braunschweig, D-38106 Braunschweig, Germany.

[2] To whom correspondence should be addressed: Center for Metals in Biology, School of Molecular & Microbial Sciences, Cooper Rd., Bldg76, Brisbane, Qld 4072, Australia. Fax: 61-7-3365-4620; E-mail: u.kappler@uq.edu.au.

arise from heterogeneity related to the modification of the cysteine ligand of the SoxA active site heme.

Based on the crystal structures, a SoxAX reaction mechanism has been proposed (5, 14) that leads to the formation of a new S–S bond between the thiosulfate ion and a conserved cysteine residue present in the SoxY subunit of the SoxYZ carrier protein (Equation 1).

$$\text{SoxZY-SH} + \text{S-SO}_3^{2-} + 2\ \text{ferricytochrome } c \rightarrow \text{SoxZY-S-S-SO}_3^{-} + 2\ \text{ferrocytochrome } c \quad \text{(Eq. 1)}$$

This reaction requires the simultaneous transfer of two electrons from the substrates to SoxAX, which then mediates consecutive single electron transfer to two ferricytochromes *c*. The obvious candidate redox centers for the electron transfer reaction are the two heme groups present at the active site of both di- and triheme SoxAX proteins.

Until recently, only a single heme redox potential had been reported for both the triheme *Rhodovulum sulfidophilum* SoxAX protein and the *S. novella* diheme SoxAX protein (1, 14), despite the fact that they contain three and two heme cofactors, respectively. Given the differences in axial ligation (His/Met and His/Cys), at least two well separated heme redox potentials should be present (19).

It has also been suggested that the SoxAX mechanism might be similar to that found in rhodaneses (EC 2.8.1.1) and could involve a temporary dissociation of the cysteine ligand from the active site SoxA heme group (14).

Together, these observations raise several questions about the reaction catalyzed by SoxAX and about how reaction specificity can be maintained if the presence of some sulfur compounds already leads to modifications of the SoxA subunit. It is also unclear how the SoxAX redox centers participate in catalysis (14, 16).

In the present study we have reassessed the properties and types of redox centers present in the diheme SoxAX protein from *S. novella*, which has lead to the identification of an additional redox active metal center in SoxAX. This Cu^{II} center is important for SoxAX reactivity toward sulfur compounds because it enhances SoxAX activity in our newly developed SoxAX assay, which is the first assay reported for an individual component of the Sox multienzyme complex.

EXPERIMENTAL PROCEDURES

Protein Production and Purification—Recombinant SoxAX was produced from either periplasmic or whole cell extracts as in Ref. 20. For cytoplasmic production of recombinant SoxYZ, the *S. novella soxYZ* genes (GenBank™ AF139113) were amplified by PCR using Phusion Polymerase (Finnzymes) and primers ExsoxYpProF (*AAAA GGATC C*AC CGA GGA GAT GGT CGC G) and ExSoxZR (*AAAA TCTAGA* TCA GGC GAC GGT GAG CTT G) and cloned into the BamHI and XbaI restriction sites of pProex-HTB (Invitrogen), resulting in pProex-SoxYZ. SoxYZ was expressed in *Escherichia coli* BL21 in a complex autoinduction medium (Novagen) at 20 °C. SoxYZ was purified using a combination of affinity chromatography (HisTrap 5 ml, GE Healthcare) and cation exchange (SP Sepharose, GE Healthcare). Purified SoxYZ was stored in 20 mM Tris-Cl (pH 7), 2 mM dithiothreitol.

Metal Binding Assays—Binding of metals to purified SoxAX was essentially carried out as in Ref. 21. To 400 μl of purified SoxAX (100 μM), a concentrated Cu^{II} chloride solution was added (final protein to metal ion ratio: 1:3). The samples were incubated on ice for 30 min followed by exhaustive dialysis against 20 mM Tris-HCl (pH 7.8) at 4 °C. Bovine serum albumin and horse heart cytochrome *c* were used as control proteins, and solutions of Mn^{II}, Mg^{II}, Zn^{II}, and Ni^{II} salts were used to test the specificity of copper binding to SoxAX. Metal ion content was determined by inductively coupled plasma mass spectrometry at the ENTOX Center at the University of Queensland.

Redox Potentiometry—Titrations were performed inside an anaerobic glovebox ($O_2 < 10$ ppm) using previously reported methods (22). The titration solution comprised 1.5 ml of 1–3 μM protein in 50 mM MES[3] (pH 6), phosphate (pH 7), or Tris (pH 8) plus 10 mM NaCl. The redox reactions were facilitated by a mixture of inorganic mediator titrants (each 10 μM) described previously (22). The reductant was an approximately 5 mM solution of $Na_2S_2O_4$ (freshly prepared) or 7 mM Ti^{III} citrate (23) for very low potential work, and the oxidant was approximately 5 mM $Na_2S_2O_8$.

Wavelengths at which there was a maximum absorbance change upon reduction/oxidation were chosen, and a cross-section of potential/absorbance pairs (*E* and *A*) was selected and fitted to Equation 2. Formal potentials (*E*1° and *E*2°) and limiting absorbance values (A_{ox} and A_{red}) for the couple were obtained from the fit.

$$Abs = \frac{(A_{ox}10^{(E - E1°)/59} + A_{red})}{1 + 10^{(E - E1°)/59}} + \frac{(A_{ox}10^{(E - E2°)/59} + A_{red})}{1 + 10^{(E - E2°)/59}} \quad \text{(Eq. 2)}$$

The potential *E*1 was obtained directly from the high potential subset of data using only the first term of Equation 2. However, *E*2 was on the verge of the low potential limit set by the reductant Ti^{III} citrate ($Ti^{IV/III}$ $E^{o\ -}$480 mV at pH 7) (23), and 100% reduction of the protein could only be obtained by the addition of a large excess of reductant, which resulted in severe optical interference from the Ti^{III} citrate complex. To enable a meaningful fit to Equation 2, it was assumed that the extinction coefficients of both high and low potential ferrous and ferric hemes (A_{ox} and A_{red}) were the same, and thus each sigmoidal component was of equal amplitude.

EPR Spectroscopy—Continuous wave X-band (~9 GHz) EPR spectra of "as prepared" and copper-loaded SoxAX (0.4 mM SoxAX in 50 mM Tris, pH 7.8, 50% glycerol) were recorded on a Bruker Biospin Elexsys E580 EPR spectrometer as previously described (1). EPR spectra of copper-loaded SoxAX after incubation with 1 mM reduced glutathione were collected at 60 K.

Simulation of the continuous wave EPR spectra was performed with version 1.1.4 of the XSophe-Sophe-XeprView software suite using matrix diagonalization in conjunction with the mosaic misorientation line width model and a quadratic variation of the Hooke and Jeeves optimization algorithm (24). A

[3] The abbreviations used are: MES, 4-morpholineethanesulfonic acid; NIR, near infrared; NHE, normal hydrogen electrode; MCD, magnetic circular dichroism.

distribution of g and A values was employed to account for the line width variation in the anisotropic spectra.

$$H = \beta_e \underline{B} \cdot g \cdot \underline{S} + \underline{S} \cdot A_{Cu} \cdot \underline{I_{Cu}} - g_n \beta_n \underline{B} \cdot \underline{I_{Cu}} + \sum_{k=1}^{3,4} \underline{S} \cdot A_{N_k} \cdot \underline{I_{N_k}} - g_n \beta_n \underline{B} \cdot \underline{I_{N_k}} \quad \text{(Eq. 3)}$$

The simulations used the spin Hamiltonian (Equation 3), where β_e and β_n are the Bohr and nuclear magnetons, respectively, B is the static magnetic field, g and A are the 3×3 electron Zeeman, ^{63}Cu and ^{14}N hyperfine interaction matrices, respectively, S and I are the electron and nuclear spin vector operators, and g_n is the nuclear g value for the ^{63,65}Cu ($I = 3/2$) nuclei and the ^{14,15}N nuclei, and all naturally occurring isotopes of copper (^{63}Cu, I = 3/2, $g_n = -1.4822$, 69.17% abundant; ^{65}Cu, I = 3/2, $g_n = -1.5878$, 30.83% abundant) and nitrogen (^{14}N, I = 1, $g_n = 0.40376$, 99.632% abundant; ^{15}N, I = 1/2, $\mu = 0.56638$, 0.368% abundant) are taken into account.

EPR Redox Titration—X-band EPR spectra were obtained at 11 K as described above by treating individual 300-μl samples of 100 μM SoxAX (pH 7) with the following titrants until the indicated equilibrium potentials were reached: $K_3[Fe^{III}(CN)_6]$ (+372 mV *versus* NHE, fully oxidized), $[Co^{II}$ (diaminosar)$](ClO_4)_2$ (25) (−331 mV *versus* NHE, one-heme reduced, data not shown) and Ti^{III}-citrate (−512 mV *versus* NHE, two-heme reduced). A redox titration of copper-loaded, 100 μM SoxAX (pH 8) was carried out using the mediators and procedures specified above. The X-band EPR spectra were collected at 130 K.

MCD Spectroscopy—Total and differential circularly polarized light intensity were measured simultaneously using a single beam instrument consisting of a Jobin/Yvon 750S monochromator, a photo-elastic modulator (Hinds PEM II/IS42), an Oxford Instruments Spectromag 7T superconducting magnet, and either a S-5 photomultiplier (Hamamatsu R7459; 300–700 nm) or an InGaAs photodiode detector (UDT sensors 3 mm; 700–1700 nm) (26). The samples contained 20 mM Tris-Cl (pH 8) and 60% (v/v) glycerol as a glassing agent. Sample concentrations were varied between 25 and 100 μM for detection of signals in the visible and infrared range, respectively. The samples for the detection of infrared signals were prepared using deuterium oxide based buffers. The spectra were routinely measured at 1.7 K and 7.0 Tesla.

SoxAX Activity Assays—SoxAX activity assays routinely contained 20 mM MES (pH 6) or 20 mM Tris-acetate buffers, 1 mM reduced glutathione (freshly prepared stock solution (100 mM, pH 7) was used for ~30 min following preparation), 0.04 mM cytochrome *c* horse heart. The reaction was monitored at 25 °C and 550 nm.

One unit of enzyme activity refers to the amount of enzyme required to reduce 1 μmol cytochrome *c*/min. pH values above 8 and free Cu^{II} ions were found to enhance the background rate of glutathione dependent cytochrome *c* reduction.

Optical spectra of 9.1 μM SoxAX (as prepared and copper-loaded) in the presence of 1 mM glutathione or 60 μM SoxYZ were recorded between 250 and 750 nm repeatedly for up to 2.5 h. Reductant was removed from the SoxYZ preparation immediately prior to the experiment using a PD-10 column. Buffer containing 2 mM dithiothreitol was treated similarly and used as a negative control.

TABLE 1
Redox potentials of SoxAX (mV *vs.* NHE) obtained from optical potentiometry
The uncertainties in each potential are estimated to be ± 10 mV.

	Copper-loaded		Copper-free	
	E1	*E2*	*E1*	*E2*
pH 6	+184	−430	+181	−424
pH 7	+184	−455	+183	−479
pH 8	+180	−486	+174	−507

RESULTS

Redox Potentials of the SoxAX Heme Groups—A peculiar feature of SoxAX proteins is that regardless of whether there are two or three heme groups present in the protein, only a single heme-dependent redox potential had been derived from optical redox titrations of the native, wild type SoxAX proteins (*R. sulfidophilum* SoxAX ~180 mV (14), *S. novella* native SoxAX ~ 104 mV at pH 7 (1)) in studies carried out before this work began. To establish whether both heme groups were reduced at the same potential or not, we carried out EPR redox titrations. However, although this allowed us to establish a potential of ~223 ± 10 mV at pH 7 for the His/Met-ligated heme (LS3) of the SoxX subunit, the EPR signal of the His/Cys-ligated heme could not be completely reduced in a potential range between −400 and +300 mV *versus* NHE using sodium dithionite as the reductant.

We therefore re-evaluated the redox properties of the diheme *S. novella* SoxAX using titanium citrate as a reductant, which led to the discovery of two heme-dependent redox potentials, *E*1 and *E*2. The higher heme redox potential (*E*1) was found to be pH-independent in the range $6 < pH < 8$, which is typical for His/Met-ligated cytochromes *c*. The observed *E*1 potential (+183 ± 10 mV, pH 7) is somewhat lower than that of analogues such as cytochrome *c* (horse heart, +260 mV) (27). In contrast, the second potential (*E*2) was found to be extremely low (−479 ± 10mV pH 7) (Table 1). This potential decreased slightly with an increase in pH but not enough to be associated with proton coupled electron transfer (−59 mV/pH).

Three distinct stages can be distinguished during optical redox titrations of SoxAX (Fig. 1*A* and supplemental Fig. S1). At high potential the α-band of both hemes is absent. Upon reduction of one of the hemes, the α-band and Soret band grow in intensity before remaining unchanged between +100 and −400 mV *versus* NHE. Within this initial plateau region the spectrum (Fig. 1 and supplemental Fig. S1) is a composite of a ferric and a ferrous heme. At very low potentials, the α-band and Soret band grow once more in intensity, indicating reduction of the second heme (Fig. 1*A*). This is accompanied by a noticeable narrowing of the spectral bands as the broader ferric heme maxima in the regions 500–600 and 400–450 nm vanish.

These results were confirmed using EPR spectroscopy. The ferricyanide-oxidized protein (Fig. 1*B*) gave resonances from both ferric hemes in addition to Cu^{II} hyperfine resonances of which the perpendicular resonance ($g_\perp = \sim 2.04$, 320 mT) is

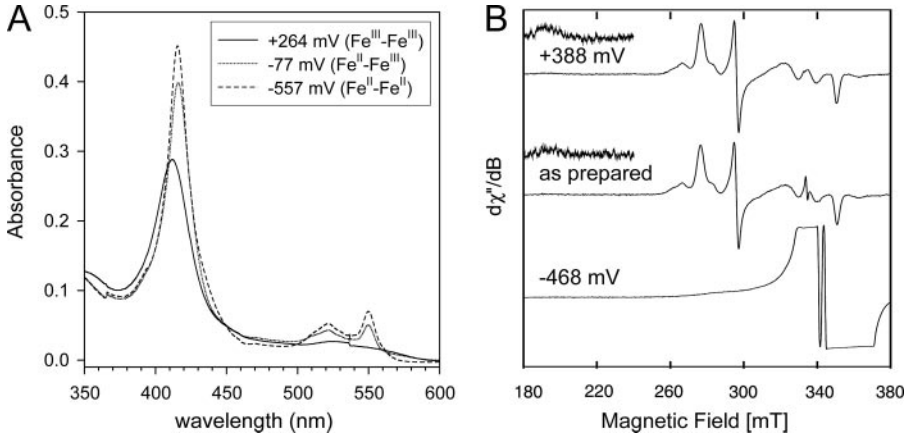

FIGURE 1. **Electronic absorption and EPR spectra of SoxAX.** *A*, electronic spectra of fully oxidized (*solid line*), single electron reduced (*dotted line*), and fully reduced (*dashed line*) SoxAX (2.6 μM) at pH 8. *B*, X-band EPR spectra of fully oxidized (+388 mV, ν = 9.3759 GHz), as prepared (single electron reduced, ν = 9.3776 GHz) and fully reduced (−468 mV, ν = 9.3759 GHz) SoxAX (100 μM, pH 7, 11 K). The potentials at which the protein was poised in each case are shown. The g = 3.5 resonance from LS3 has been scaled by a factor of 10 for the fully oxidized and as prepared samples.

clearly resolved. The only band of significant intensity from the high potential heme (*E1*, EPR signal: LS3) appears at g = 3.5 (~190 mT, expansion; Fig. 1*B*). This peak is much weaker in the as prepared sample (Fig. 1*B*, *middle spectrum*), indicating that the protein is mostly in its one-electron reduced form. Upon reduction with excess Ti^{III} citrate, all heme and copper EPR signals vanish, and only resonances caused by Ti^{III} (g = 1.953, ~342 mT) remain (Fig. 1*B*). The optical and EPR redox titrations thus confirm that the highly anisotropic LS3 spectrum corresponds to that of the high potential heme *E1*.

The finding of an extremely low redox potential for the His/Cys-ligated heme present in the *S. novella* diheme SoxAX protein is not unprecedented; a similarly low redox potential (−32 ± 15 mV, pH 7) has just recently been reported for the active site SoxA heme of the triheme SoxAX protein from *Paracoccus pantotrophus* (28), and our results confirm that the low redox potential of the SoxA active site heme is a property of both di- and triheme SoxA proteins. Other His/Cys-ligated heme groups also have low redox potentials; a redox potential of −160 ± 10 mV (pH 7) was determined for a His/Cys-ligated heme from *R. sulfidophilum* (29), and the membrane-bound, His/Cys-ligated DsrJ cytochrome was still unreduced at a potential of −400 mV (30). The low redox potential of the His/Cys-ligated SoxA heme suggests that this heme group does not participate in electron transfer in SoxAX, and this has implications for the proposed SoxAX reaction mechanism that requires the transient storage and transfer of two electrons (Equation 1).

SoxAX Is a Cu^{II}-binding Protein—All published EPR spectra of SoxAX proteins contain an axially symmetric Cu^{II} signal that has usually been interpreted as deriving from adventitious copper (1, 18). Metal analysis of purified recombinant SoxAX showed a copper content of 15–25%, whereas a sulfite dehydrogenase that is purified using a similar combination of column steps and buffer systems (20) only contained ~5% Cu. We therefore assessed the ability of SoxAX to bind copper relative to cytochrome *c* and a known copper-binding protein, bovine serum albumin. Both bovine serum albumin (1.2 copper atoms/molecule) and SoxAX (1.05 ± 0.014 copper atoms/molecule) bound one equivalent of copper, whereas horse heart cytochrome *c* (0.03 copper atoms/molecule) had only retained negligible amounts of copper as a result of the treatment. Copper levels in buffer samples were 2.5 and ~350 times lower that those of the untreated and copper-loaded protein samples, respectively, excluding the buffer as a source of the copper detected in SoxAX preparations. Repetition of the treatment did not result in an increase of the amount of copper bound to SoxAX. Metal binding was specific for copper because Mn^{II}, Mg^{II}, Zn^{II}, and Ni^{II} were not retained by SoxAX at significant levels. The presence or absence of copper in SoxAX samples was found to have no effect on the heme redox potentials (Table 1). No optical bands associated with the Cu^{II} center could be detected, which is not surprising given the competing heme chromophores. The redox potential of the copper center present in SoxAX was determined by EPR redox titration and found to be +196 ± 18 mV *versus* NHE at pH 8 (supplemental Fig. S2).

EPR Spectroscopy of Copper-loaded SoxAX—In previous studies of SoxAX proteins four separate sets of low spin ferric heme EPR signals have been identified, LS1a,b, LS2, and LS3 (1,17,18). An EPR spectrum (recorded at 2 K) of copper-loaded SoxAX (Fig. 2*a*) revealed resonances from LS1 and LS2, both of which are associated with the His/Cys-ligated SoxA heme as well as EPR signals near g = ~2 (316–343 mT), which is typical of a magnetically isolated Cu^{II} center. The LS1a and LS1b centers describe a small heterogeneity in g_z and are simulated separately (1, 18). The low field copper parallel hyperfine resonances overlay those from LS1 and LS2. EPR spectra were then recorded at 60 and 130 K to resolve the resonances from just the Cu^{II} center. However, both at 60 K (Fig. 2, *spectra b* and *c*) and at 130 K (data not shown) SoxAX EPR spectra still show resonances from LS1, LS2, and the Cu^{II} center, although the intensities of the Cu^{II} resonances are significantly larger than those for the heme signals. Thus, both conformations of the His/Cys-ligated *E2* heme (LS1 and LS2) must have long spin lattice relaxation times (T_1). A comparison of the line widths of the g = 1.912 resonance belonging to LS2 in the as prepared sample and Cu^{II}-loaded SoxAX in Fig. 2 (*spectrum b*, $\Delta B_{1/2}$ = 3.22 mT; and *spectrum c*, $\Delta B_{1/2}$ = 4.22 mT), respectively, suggests the presence of a dipole-dipole interaction between the Cu^{II} and the LS2 low spin Fe^{III} center. This indicates that the Cu^{II} and LS2 heme centers must be within ~10–15 Å of each other.

Subtraction of the data recorded at 60 K of as prepared SoxAX (Fig. 2, *spectrum b*) from that of the copper-loaded SoxAX sample (Fig. 2, *spectrum c*) yields the spectrum associated with the Cu^{II} center (Fig. 2, *spectrum d*). This spectrum is typical of a tetragonally distorted square planar Cu^{II} center and also shows partially resolved nitrogen superhyperfine coupling

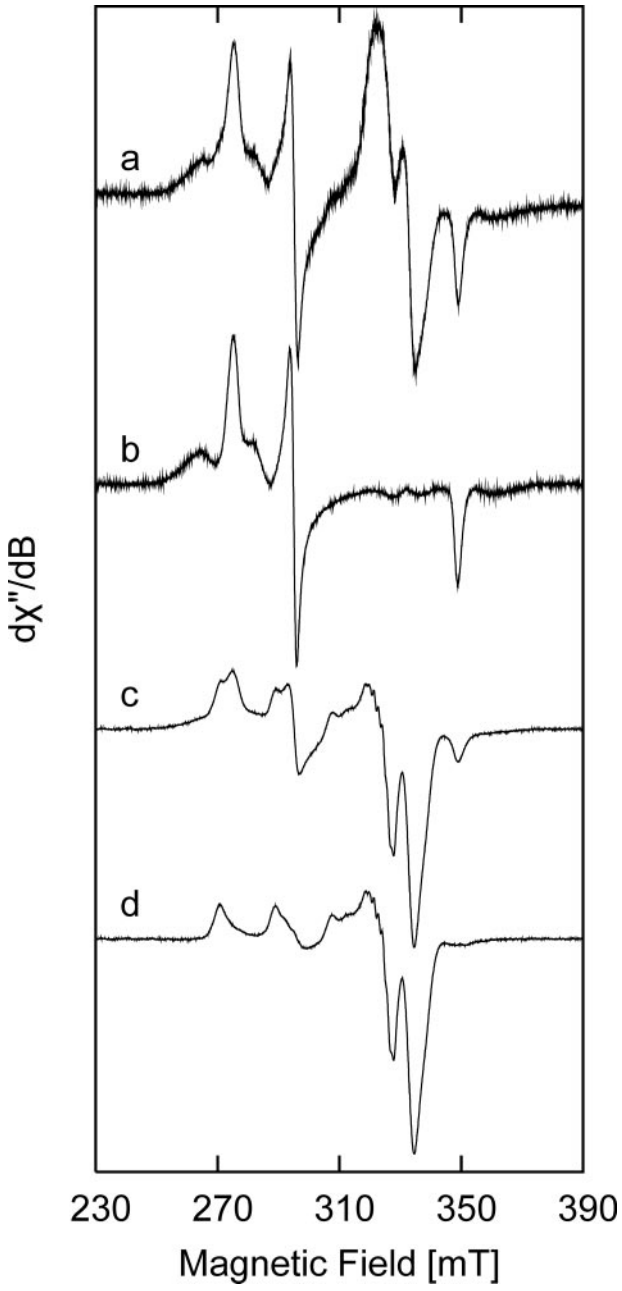

FIGURE 2. **X-band EPR spectra of SoxAX and Cu^{II} loaded SoxAX.** *Spectrum a*, Cu^{II} loaded SoxAX, T = 2.07K, ν = 9.3398 GHz; *spectrum b*, SoxAX, T = 60K, ν = 9.3344 GHz; *spectrum c*, Cu^{II}-loaded SoxAX, T = 60.0K, ν = 9.3392 GHz; *spectrum d*, difference spectrum subtraction of *spectrum b* from *spectrum c*.

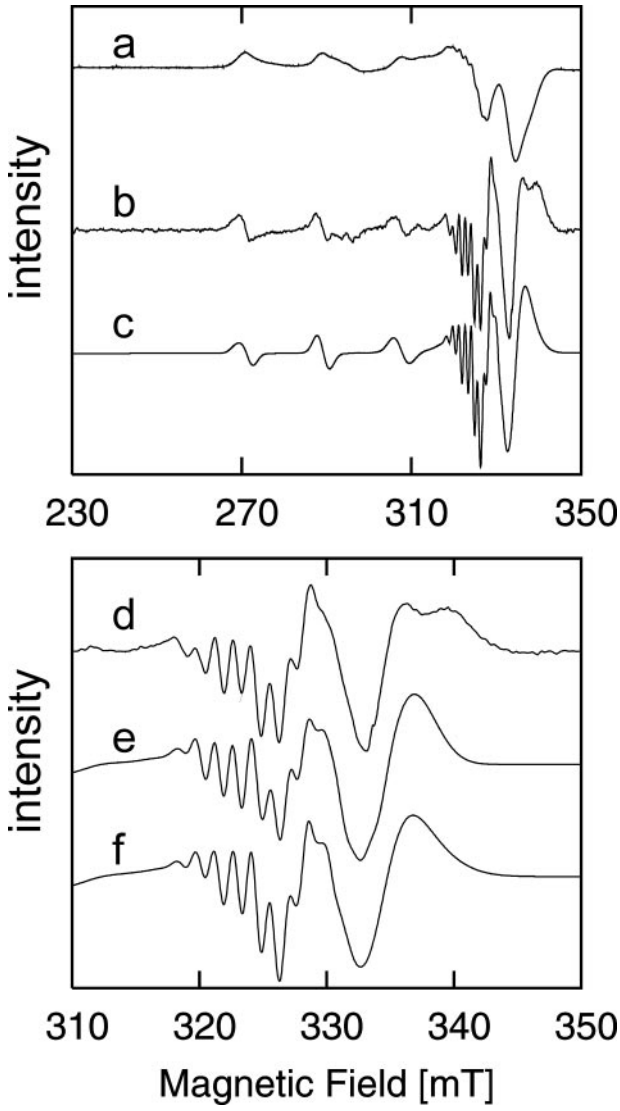

FIGURE 3. **Simulation of copper-loaded SoxAX EPR Spectra.** *Spectrum a*, EPR spectrum of the Cu^{II} center (Fig. 2, *spectrum d*). *Spectrum b*, Fourier filtered second derivative experimental spectrum. *spectra d–f*, expansion of the perpendicular region. *Spectrum d*, experimental data; *spectra e* and *f*, simulated spectra assuming superhyperfine coupling to three (*spectrum e*) and four (*spectra c* and *f*) nitrogen nuclei, respectively. Both simulations (*spectra e* and *f*) lack the resonance at high field (339.5 mT) and the small resonances at 292.3 and 295.0 mT (*spectrum b*), which probably arise from a slightly imperfect subtraction of the as prepared from the copper-loaded SoxAX spectrum.

from nitrogen nuclei in the perpendicular region. Differentiation together with Fourier filtering (Hamming function) improves the spectra resolution (Fig. 3). Simulation (24) of the second derivative spectrum of the experimental data assuming three or four ^{14}N nuclei ($I = 1$), an orthorhombic spin Hamiltonian (Equation 3), and the following parameters (3N: g_x 2.0396; g_y 2.0476; g_z 2.2350; (^{63}Cu) A_x 18.71; A_y 22.03; A_z 187.26; (^{14}N 2 magnetically equivalent nuclei (2 MEq.)) A_x 12.52; A_y 8.19; A_z 1.45; (^{14}N) A_x 16.30; A_y 6.93; A_z 5.0; 4N: g_x 2.0396; g_y 2.0465; g_z 2.2350; (^{63}Cu) A_x 19.49; A_y 20.71; A_z 187.26; (^{14}N 2 MEq.) A_x 12.23; A_y 8.20; A_z 1.45; (^{14}N 2 MEq.) A_x 15.44; A_y 6.47; A_z 5.0; units for A are 10^{-4} cm^{-1}) yields the spectra shown in Fig. 3 (*spectra c*, *e*, and *f*, respectively). The least squares error (24) for these simulations are 0.0719 and 0.0618, respectively, and consequently, the simulations do not allow us to distinguish between three and four nitrogen atoms coordinated to the Cu^{II} center. In the absence of resolved nitrogen superhyperfine coupling, Blumberg Peisach plots that correlate $g_{\|}$ and $A_{\|}$ with coordination spheres (3N1O, 4N, 2N2O, etc.) have been exploited to identify the ligating atoms coordinated to Cu^{II} ions. Using the Blumberg Peisach plots, the $g_{\|}$ and $A_{\|}$ values for the Cu^{II} center in SoxAX indicate either a neutral [Cu(3N1O)] or anionic $[Cu(4N)]^-$ complex.

Preliminary three pulse ESEEM and HYSCORE spectra measured at $g_{\perp}$ reveal nitrogen superhyperfine coupling to N_{ϵ} from a single histidine residue. Consequently, the remaining nitrogen atoms must arise from deprotonated peptide amide

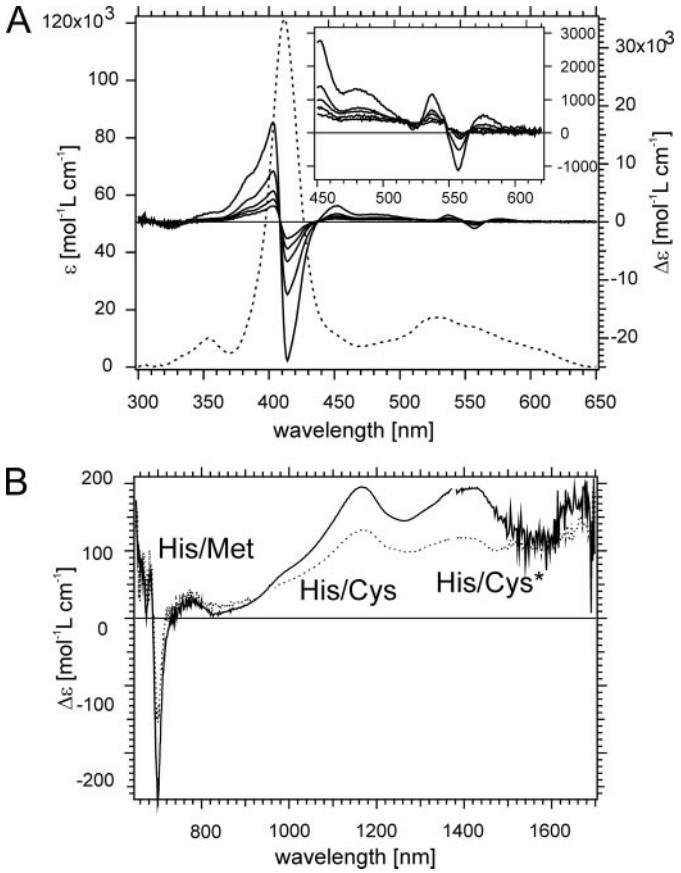

FIGURE 4. **UV-visible and NIR MCD spectra of as prepared *S. novella* diheme SoxAX.** *A*, UV-visible MCD spectrum. *Dotted trace*, SoxAX electronic absorption spectrum. *Solid traces*, low temperature SoxAX MCD spectra recorded at 7.0 Tesla and temperatures of 2, 10, 20, 30, and 50 K. Sample concentration, 25 μM; path length, 1 mm. *Inset*, enlargement of 450–620 nm region of the MCD spectra. *B*, NIR MCD spectra of as prepared SoxAX (*solid line*) and copper-loaded SoxAX (*dotted line*). Features arising from heme ligands are labeled in the figure.

nitrogens to reproduce the charge predicted by the Blumberg Peisach plots.

MCD Spectroscopy and the Ligand Field of the Heme Cofactors—Together with EPR, MCD spectroscopy is an established method for investigating the heme ligand field in cytochromes (31). The MCD spectra of the *S. novella* diheme SoxAX (UV-visible, 300–650 nm) are typical of low spin ferric heme and are similar to what has been observed previously for the triheme SoxAX from *R. sulfidophilum* (18) (Fig. 4). As noted previously (18), the intensity of the Soret band is low. There is no evidence for the presence of high spin or ferrous hemes from the temperature-dependent spectra magnetization curves of the SoxAX Soret band (403 nm). For $S > 1/2$ ground states with a zero field splitting, the temperature-dependent magnetization curves would be expected to be nested (32) rather than overlaying each other as shown in supplemental Fig. S3. Assuming an *x-y* polarized transition, a calculated magnetization curve can be fitted to an isolated $S = 1/2$ Kramer's doublet with a $g_z = 2.512$ (g_x and g_y are insensitive to this fit).

A comparison of the MCD spectra of as prepared and copper-loaded SoxAX in both the UV-visible and the NIR region does not show significant differences (Fig. 4). In the NIR, the sharp negative feature has been assigned as a *z*-polarized ligand to metal charge transfer transition involving a methionine sulfur and Fe^{III} (33, 34). The observed positive MCD in the range 800–1600 nm is due to ligand to metal charge transfer transitions of low spin ferric heme (18). The peak at 1160 nm has been assigned to the ligand to metal charge transfer transition of the His/Cys-ligated heme (35), whereas the positive MCD signal at 1250–1500 nm has been proposed to be associated with the LS2 EPR signal (18), which is thought to be due to the modification of the heme-ligating cysteine to a cysteine persulfide.

Application of a standard Taylor analysis to the *g* values of the SoxA heme (supplemental Table S1) suggests a d_{xy} ground state with a *z*-axis in the plane of the heme if the axis system adheres to $|v/\Delta| < 2/3$ for tetragonal (Δ) and rhombic (v) parameters (1, 36). Because this is an unusual electronic ground state, referred to as a "type III" heme found for some cytochromes *d* (31), we re-examined the assumptions in the analysis in detail. We have found that the use of anisotropic orbital reduction parameters was necessary to give v/Δ values appropriate for the expected type II heme and a d_{yz} ground state (supplemental Table S1). Similar observations have been made for a number of low spin ferric hemes (31), where $|v/\Delta|$ has been found to be $>2/3$ in cases that unambiguously have a d_{yz} ground state.

The LS1a,b and LS2 centers thus display "normal rhombic" *g* values for a low spin ferriheme that have been interpreted as indicative of the axial ligands being in a near parallel rather than perpendicular orientation (37).

Empirical relationships have been found for the energy of the $a_{1u} \rightarrow d_{yz}$ porphyrin to metal charge transfer transition as a function of the axial ligands (38). These predict the charge transfer transition of a His/Met-ligated heme to occur at 1835 nm and that of a His/Cys-ligated heme at 1176 nm. This latter value correlates very well with the 1160-nm peak seen in Fig. 4, whereas the former is out of the range of our detector. The peak at ~1400 nm, which has been proposed to correspond to the His/Cys persulfide-ligated heme (18) (Fig. 4), then implies an energy parameter of $E_l = 3950\ cm^{-1}$. However, the larger values of Δ and v for a d_{yz} ground state of LS2 (supplemental Table S1) (33) predict that E_{CT} for the His/Cys persulfide ligand should occur at higher energies and shorter wavelengths than those observed for the His/Cys ligand center (1400 nm), which is opposite to what has been previously proposed (18).

SoxAX Has Glutathione: Cytochrome c Oxidoreductase Activity—The proposed reaction of SoxAX (Equation 1) consists of the formation of a disulfide bridge between a cysteine residue of the SoxYZ protein and the thiosulfate sulfane sulfur, which liberates two electrons that are then transferred to two molecules of ferricytochrome *c* (5, 14). To date, this reaction has not been observed in isolation. An *in vitro* assay for this reaction requires a suitable electron acceptor and the presence of two sulfur compounds that can undergo S–S bond formation. Ideally, one of the two sulfur compounds should mimic the C-terminal GGCGG amino acid motif of the SoxY protein that has been shown to be the site of the heterodisulfide bond formation (10).

We had noted previously that incubation of as prepared SoxAX with reduced glutathione led to a reduction of the pro-

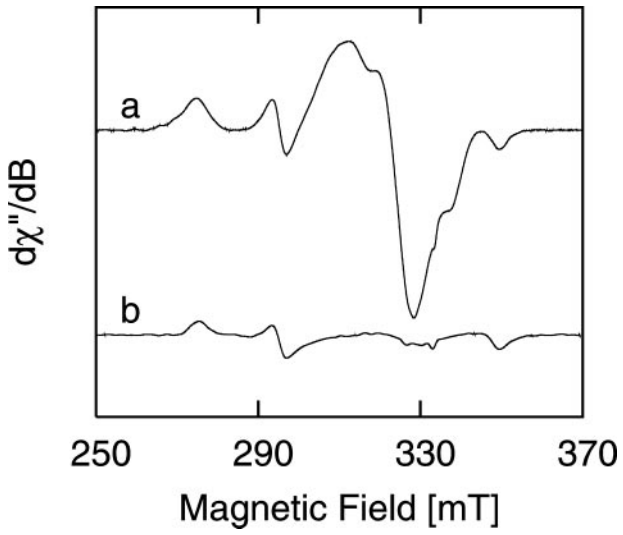

FIGURE 5. **EPR spectrum of copper-loaded SoxAX after treatment with 1 mM glutathione, ν = 9. 3532 GHz, T = 130K.** *Spectrum a*, untreated SoxAX sample. *Spectrum b*, glutathione-treated SoxAX sample.

tein as judged by its color and optical spectra.[4] Using 9.1 μM solutions of purified SoxAX and 1 mM glutathione (ratio of ~1:100), copper-loaded SoxAX (0.3 μM/min) was reduced 7.5 times faster than as prepared SoxAX (0.04 μM/min), indicating that copper enhances the reactivity of SoxAX towards sulfur compounds. Moreover, we were able to show by EPR that incubation with glutathione reduces the SoxAX copper center, confirming that the copper ion participates in the reaction (Fig. 5). This reaction is similar to what we have observed using a recombinant form of the *S. novella* SoxYZ carrier protein (Equation 1) that is thought to be the native reaction partner of SoxAX. Like glutathione, purified SoxYZ was able to reduce copper-loaded SoxAX when the two purified proteins were mixed in a ratio of 6:1 (0.049 μM/min), indicating the biological relevance of the observed enzymatic activity of SoxAX with glutathione. Glutathione is a very good model compound for the SoxYZ-based reaction because it is a small, highly mobile tripeptide with the cysteine in the central position. In the SoxYZ protein, the reactive cysteine present in SoxY is located at the very C terminus of the protein, in a conserved GGCGG amino acid motif that has been shown to be hypermobile and capable of assuming a variety of conformations (39).

Based on these observations, an assay system for SoxAX that uses glutathione as the sulfur compound and horse heart cytochrome *c* as the electron acceptor was devised (Fig. 6). Cysteine or glutathione in combination with thiosulfate were also tested but were found to reduce the horse heart cytochrome *c* at a high rate in the absence of SoxAX. In this assay system, copper-loading enhanced SoxAX activity 14 times from 0.124 unit/mg to 1.54 units/mg at pH 6.2, indicating again the significance of the copper center for SoxAX reactivity. The reaction rate saturated at higher SoxAX concentrations when assays were carried out with increasing amounts of copper-loaded SoxAX (Fig. 6). We propose that in the assay system GSSG is formed instead of SoxZY-S–S-SO_3^- (Equations 1 and 4).

[4] U. Kappler, unpublished observations.

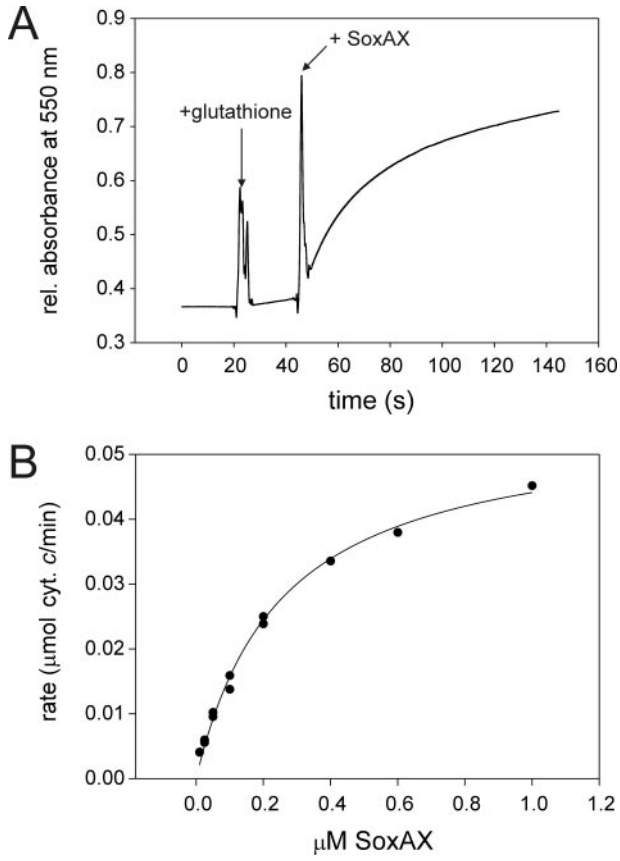

FIGURE 6. **Reaction of SoxAX in the glutathione-based assay system.** *A*, typical reaction of SoxAX with glutathione and horse heart cytochrome *c*. 0.4 μM SoxAX were present in the assay shown. After the addition of glutathione to the reaction mix containing buffer and cytochrome *c*, a background rate of cytochrome *c* reduction is obtained that is subtracted from the reaction rate obtained after addition of SoxAX to the assay. *B*, dependence of the rate of catalysis (μmol cytochrome *c* reduced/min) on the amount of SoxAX (μM) present in the assay system.

$$2GSH + 2\ \text{ferricytochrome } c \rightarrow GSSG + 2\ \text{ferrocytochrome } c \quad \text{(Eq. 4)}$$

Apparent K_m values for reduced glutathione were 0.49 ± 0.12 and 0.19 ± 0.028 mM at pH 6 (20 mM MES buffer) and pH 7 (20 mM Tris-acetate buffer), respectively, with corresponding apparent k_{cat} values of 8.72 ± 0.84 and 5.7 ± 0.25 s^{-1}. Assay components prepared with ultrapure water usually only give rise to very small background rates of cytochrome *c* reduction (Fig. 6*A*). However, because the assay system measures an enzymatic reaction in which metal ions play a major role in catalysis, testing for interference from free metal ions was carried out during the development of the assay. During these tests, defined amounts of free metal ions (Cu^{II}, Mn^{II}, Zn^{II}, Ag^{II}, Fe^{II}, and Mg^{II}) were added to the assay mixture instead of the SoxAX protein from concentrated stock solutions. Cu^{II} was the only metal found to interfere with the assay system; however, rates of cytochrome *c* reduction mediated by free Cu^{II} were always lower than the rates observed during enzymatic catalysis by copper-loaded SoxAX by a factor of 1.8–2 up to a concentration of 0.2 μM catalyst present in the assay. With larger amounts of SoxAX, the enzymatic reaction rate no longer depended linearly on the amount of catalyst present

(Fig. 6*B*), whereas the free Cu^{II}-mediated reaction rate continued to increase linearly.

Future work will focus on replacing the reduced glutathione with purified SoxYZ and thiosulfate. However, because purified SoxYZ is hard to obtain in the quantities necessary for enzymatic activity assays at present, reduced glutathione is a convenient and easy to use alternative for measuring SoxAX activity.

DISCUSSION

In this study we have examined the redox centers present in a diheme SoxAX protein and were able to show that the His/Cys-ligated SoxA active site heme has an extremely low redox potential, which makes it unlikely that it participates in electron transfer under physiological conditions. This then causes problems with the originally proposed SoxAX reaction mechanism (Equation 1), which leads to the formation of a S–S bond, and requires transient storage of the two electrons liberated in the reaction in the SoxAX protein. Our finding that, in addition to the two active site heme groups, SoxAX also contains a Cu^{II} redox center that enhances both its activity in a newly developed *in vitro* assay system and the transfer of electrons from a sulfur donor to SoxAX. This provides a novel perspective on the unsolved problem of how the SoxAX protein mediates the formation of an S–S bond. Copper ions are known for their reactivity toward sulfur compounds and are known to be able to catalyze S–S bond formation in proteins (40). Thus, the copper center provides at the same time a catalytic center known to be capable of catalyzing the required reaction and a solution to the problem of (transient) storage of two electrons in the SoxAX protein. It is also highly likely that not only the diheme SoxAX proteins but also the triheme SoxAX proteins bind copper, because published EPR spectra of the as prepared native *R. sulfidophilum* triheme SoxAX contain features that are not part of the heme-derived spectra (18) but are similar to those observed for the copper-loaded diheme SoxAX (Fig. 2).

Based on our experimental results, we propose that the copper center mediates the initial reaction with one of the sulfur compounds, *e.g.* thiosulfate or SoxYZ, which can then either react with the second sulfur substrate to form a S–S bond or become bound to the cysteine ligand of the SoxA heme and react subsequently with the second sulfur substrate. Both processes lead to a two electron reduction of SoxAX, with one electron being stored in the copper center (Fig. 5), the other in the SoxX heme. The observed dipole-dipole interactions between the copper center and the SoxA heme suggest that the copper center should be located at a distance of ~10 Å from the SoxA heme. At present, the location and structure of the copper-binding site are not fully defined, but our results suggest that its coordination sphere involves a single His residue and either two (and a carbonyl oxygen) or three deprotonated peptide amide nitrogens. No conserved copper-binding motifs were identified in SoxAX, and in addition, the *S. novella* SoxX protein contains only the heme-ligating His residue, whereas SoxA contains a total of only three His residues, one of which is coordinated to the SoxA heme, and based on the crystal structure of *P. pantotrophus* SoxAX (16), only one of the other two His residues is likely to be located close to the SoxA active site. This His-231 (*S. novella* SoxA numbering) is conserved in sequences closely related to *S. novella* SoxA, but its exact role in copper-binding needs to be established by further structural and/or spectroscopic studies.

To completely unravel the SoxAX reaction mechanism and to provide further evidence for the revised reaction mechanism, studies including site-directed mutagenesis of the SoxA heme and copper ligands and solution of the crystal structure of the diheme SoxAX protein will be necessary. Elucidation of the SoxAX reaction mechanism also opens up completely new possibilities for studying further reactions of the Sox multienzyme complex as details about reaction substrates and products become available.

Acknowledgment—We thank Prof. A. G. McEwan for support throughout the project.

REFERENCES

1. Kappler, U., Aguey-Zinsou, K.-F., Hanson, G. R., Bernhardt, P. V., and McEwan, A. G. (2004) *J. Biol. Chem.* **279,** 6252–6260
2. Appia-Ayme, C., Little, P. J., Matsumoto, Y., Leech, A. P., and Berks, B. C. (2001) *J. Bacteriol.* **183,** 6107–6118
3. Wodara, C., Bardischewsky, F., and Friedrich, C. G. (1997) *J. Bacteriol.* **179,** 5014–5023
4. Rother, D., and Friedrich, C. G. (2002) *Biochim. Biophys. Acta* **1598,** 65–73
5. Friedrich, C. G., Rother, D., Bardischewsky, F., Quentmeier, A., and Fischer, J. (2001) *Appl. Environ. Microbiol.* **67,** 2873–2882
6. Friedrich, C. G., Bardischewsky, F., Rother, D., Quentmeier, A., and Fischer, J. (2005) *Curr. Opin. Microbiol.* **8,** 253–259
7. Lu, W. P., Swoboda, B. E. P., and Kelly, D. P. (1985) *Biochim. Biophys. Acta* **828,** 116–122
8. Hensen, D., Sperling, D., Truper, H. G., Brune, D. C., and Dahl, C. (2006) *Mol. Microbiol.* **62,** 794–810
9. Kappler, U. (2007) in *Microbial Sulfur Metabolism* (Friedrich, C. G., and Dahl, C., eds) pp. 151–169, Springer, Berlin
10. Quentmeier, A., Hellwig, P., Bardischewsky, F., Grelle, G., Kraft, R., and Friedrich, C. G. (2003) *Biochem. Biophys. Res. Commun.* **312,** 1011–1018
11. Wodara, C., Kostka, S., Egert, M., Kelly, D. P., and Friedrich, C. G. (1994) *J. Bacteriol.* **176,** 6188–6191
12. Quentmeier, A., Kraft, R., Kostka, S., Klockenkamper, R., and Friedrich, C. G. (2000) *Arch. Microbiol.* **173,** 117–125
13. Bardischewsky, F., Quentmeier, A., Rother, D., Hellwig, P., Kostka, S., and Friedrich, C. G. (2005) *Biochemistry* **44,** 7024–7034
14. Bamford, V. A., Bruno, S., Rasmussen, T., Appia-Ayme, C., Cheesman, M. R., Berks, B. C., and Hemmings, A. M. (2002) *EMBO J.* **21,** 5599–5610
15. Klarskov, K., Verte, F., VanDriessche, G., Meyer, T. E., Cusanovich, M. A., and Van Beeumen, J. (1998) *Biochemistry* **37,** 10555–10562
16. Dambe, T., Quentmeier, A., Rother, D., Friedrich, C., and Scheidig, A. J. (2005) *J. Struct. Biol.* **152,** 229–234
17. Kappler, U., Hanson, G. R., Jones, A., and McEwan, A. G. (2005) *FEBS Lett.* **579,** 2491–2498
18. Cheesman, M. R., Little, P. J., and Berks, B. C. (2001) *Biochemistry* **40,** 10562–10569
19. Frausto da Silva, J. J. R., and Williams, R. J. P. (2001) *The Biological Chemistry of the Elements: The Inorganic Chemistry of Life*, 2nd Ed., pp. 345–369, Oxford University Press, Oxford
20. Kappler, U., and McEwan, A. G. (2002) *FEBS Lett.* **529,** 208–214
21. Swem, L. R., Kraft, B. J., Swem, D. L., Setterdahl, A. T., Masuda, S., Knaff, D. B., Zaleski, J. M., and Bauer, C. E. (2003) *EMBO J.* **22,** 4699–4708
22. Bernhardt, P. V., Chen, K.-I., and Sharpe, P. C. (2006) *J. Biol. Inorg. Chem.* **11,** 930–936
23. Codd, R., Astashkin, A. V., Pacheco, A., Raitsimring, A. M., and Enemark, J. H. (2002) *J. Biol. Inorg. Chem.* **7,** 338–350

24. Hanson, G. R., Gates, K. E., Noble, C., Griffin, M., Mitchell, A., and Benson, S. (2004) *J. Inorg. Biochem.* **98,** 903–916
25. Geue, R. J., Hambley, T. W., Harrowfiled, J. M., Sargeson, A. M., and Snow, M. R. (1984) *J. Am. Chem. Soc.* **106,** 5478–5488
26. Riley, M. J., Krausz, E. R., and Stanco, A. (2003) *J. Bioinorg. Chem.* **96,** 217
27. Myer, Y. P., Saturno, A. F., Verma, B. C., and Pande, A. (1979) *J. Biol. Chem.* **254,** 11202–11207
28. Reijerse, E. J., Sommerhalter, M., Hellwig, P., Quentmeier, A., Rother, D., Laurich, C., Bothe, E., Lubitz, W., and Friedrich, C. G. (2007) *Biochemistry* **46,** 7804–7810
29. Alric, J., Tsukatani, Y., Yoshida, M., Matsuura, K., Shimada, K., Hienerwadel, R., Schoepp-Cothenet, B., Nitschke, W., Nagashima, K. V. P., and Vermeglio, A. (2004) *J. Biol. Chem.* **279,** 26090–26097
30. Pires, R. H., Venceslau, S. S., Morais, F., Teixeira, M., Xavier, A. V., and Pereira, I. A. C. (2006) *Biochemistry* **45,** 249–262
31. Walker, F. A. (1999) *Coord. Chem. Rev.* **186,** 471–534
32. Thomson, A. J., Cheesman, M. R., and George, S. J. (1993) *Methods Enzymol.* **226,** 232
33. Gadsby, P. M. A., and Thomson, A. J. (1990) *J. Am. Chem. Soc.* **112,** 5003–5011
34. Eaton, W. A., and Hochstrasser, J. M. (1967) *J. Chem. Phys.* **46,** 2533–2539
35. Dhawan, I. K., Shelver, D., Thorsteinsson, M. V., Roberts, G. P., and Johnson, M. K. (1999) *Biochemistry* **38,** 12805–12813
36. Taylor, C. P. (1977) *Biochim. Biophys. Acta* **491,** 137–149
37. Yatsunyk, L. A., Carducci, M. D., and Walker, F. A. (2003) *J. Am. Chem. Soc.* **125,** 15986–16004
38. McKnight, J., Cheesman, M. R., Thomson, A. J., Miles, J. S., and Munro, A. W. (1993) *Eur. J. Biochem.* **213,** 683–687
39. Sauve, V., Bruno, S., Berks, B. C., and Hemmings, A. M. (2007) *J. Biol. Chem.* **282,** 23194–23204
40. Multhaup, G., Schlicksupp, A., Hesse, L., Beher, D., Ruppert, T., Masters, C. L., and Beyreuther, K. (1996) *Science* **271,** 1406–1409

Supplementary Figures and Tables

Figure S1 Redox titration curve for SoxAX at pH 8. Absorbance at 552 nm from each ferrous heme chromophore is plotted as a function of the equilibrium potential. The calculated curve is shown as a dotted line. The potentials appear in Tab. 1.

Figure S2 EPR redox titration of the SoxAX Cu center, 20 mM Tris Cl, pH 8.

Figure S3 SoxAX (as prepared) magnetisation curves at 1.6K. The data has been fitted to the equation $\Delta A = a_0 \tanh(\beta B/2kT) + a_1 B$; $a_0 = 0.0379$, $a_1 = 0.0026$, $g_{\|} = 2.51$

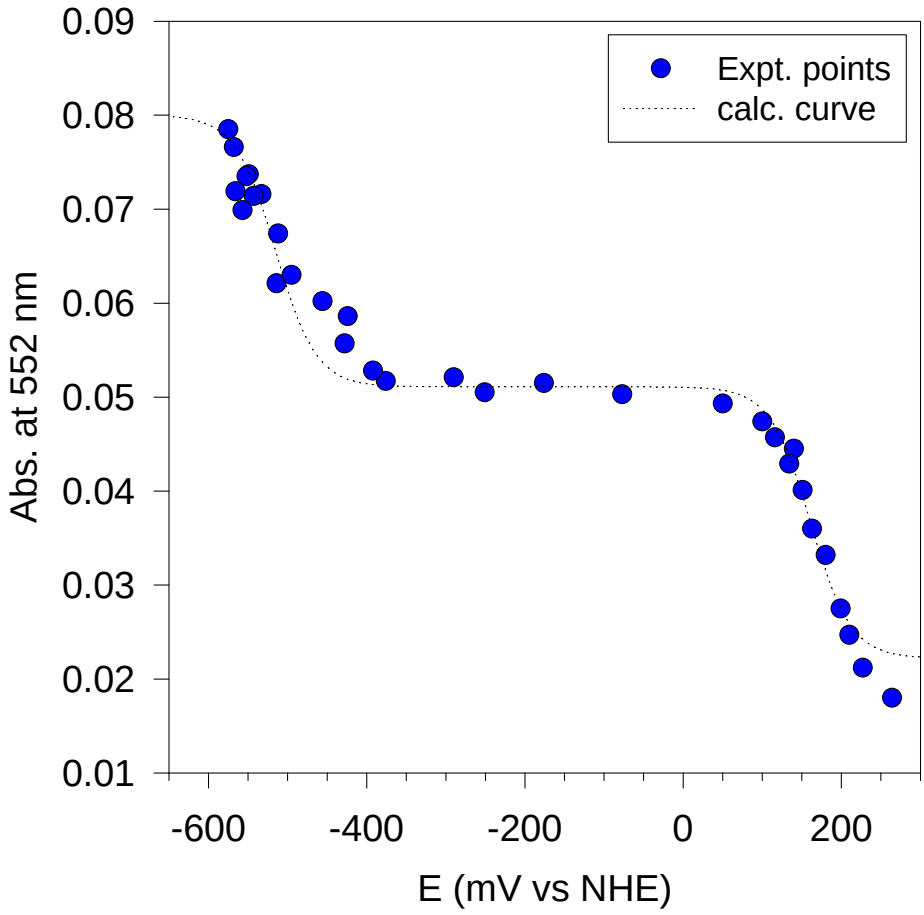
0.09
0.08
0.07
0.06
0.05
0.04
0.03
0.02
0.01
Abs. at 552 nm
-600
-400
-200
0
200
E (mV vs NHE)
Expt. points
calc. curve

Figure S1

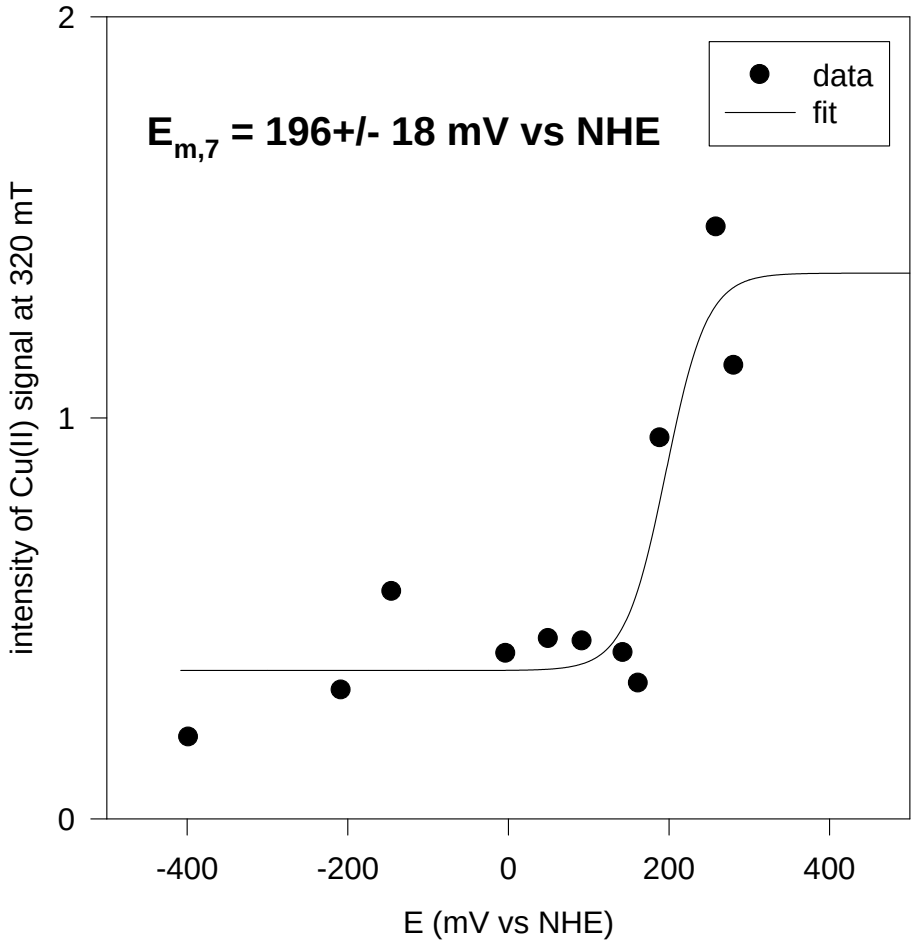
2
1
0
intensity of Cu(II) signal at 320 mT
data
fit
$E_{m,7}$ = 196+/- 18 mV vs NHE
-400
-200
0
200
400
E (mV vs NHE)

Figure S2

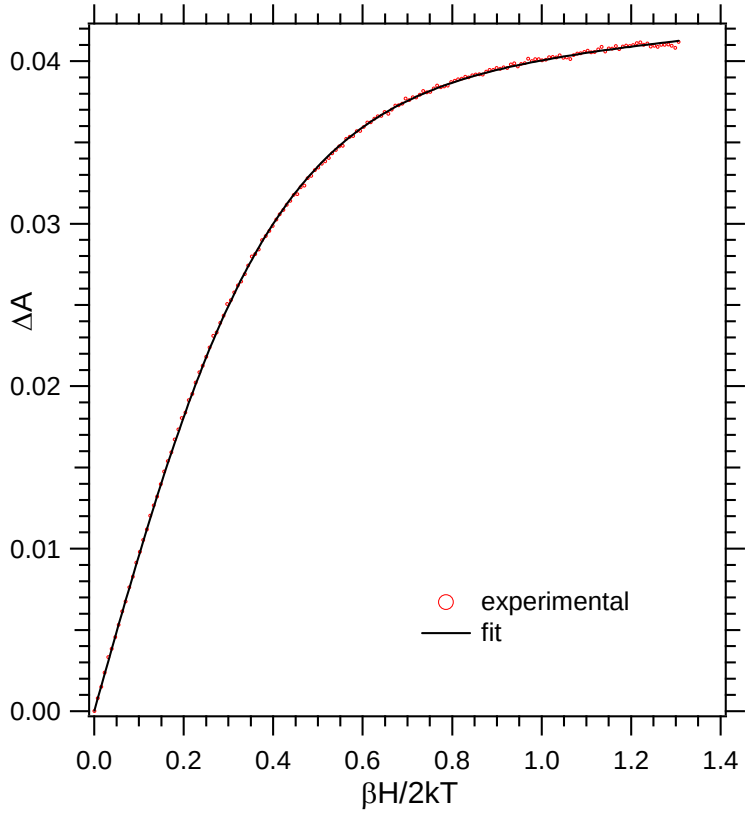
0.04
0.03
0.02
0.01
0.00
ΔA
0.0
0.2
0.4
0.6
0.8
1.0
1.2
1.4
βH/2kT
experimental
fit

Figure S3

Table S1 The *g*-values, wavefunction coefficients and ligand field parameters for the different centers in SoxAX. The wavefunction coefficients are for an electronic ground state described by $\Psi^{\pm} = a\,|yz^{\pm}> \mp i\,b\,|xz^{\pm}> \mp c\,|xy^{\mp}>$. Rows A & B correspond to different assignments of the principal axis within and perpendicular to the heme plane respectively.

center	g_x	g_y	g_z	a	b	c	N	Δ/λ	v/λ	v/Δ
LS1a A	-2.531	2.349	-1.859	0.0997	0.1367	0.9927	1.014	-4.71	-1.67	0.35
B	1.859	2.349	2.531	0.9927	0.1367	0.0997	1.014	3.61	3.88	1.07
LS1b A	-2.574	2.348	-1.835	0.1032	0.1487	0.9904	1.014	-4.47	-1.84	0.41
B	1.835	2.348	2.574	0.9904	0.1487	0.1032	1.014	3.61	3.55	0.98
LS2 A	-2.433	2.271	-1.913	0.0758	0.1100	0.9955	1.009	-5.99	-2.43	0.41
B	1.913	2.271	2.433	0.9955	0.1100	0.0758	1.009	4.82	4.77	0.99

SoxAX Cytochromes, a New Type of Heme Copper Protein Involved in Bacterial Energy Generation from Sulfur Compounds

Ulrike Kappler, Paul V. Bernhardt, James Kilmartin, Mark J. Riley, Julia Teschner, Kirsty J. McKenzie and Graeme R. Hanson

J. Biol. Chem. 2008, 283:22206-22214.
doi: 10.1074/jbc.M800315200 originally published online June 14, 2008
